

An improved mixed order model for describing thermoluminescence glow curves

M. Zahedifar* and S. Harooni

TL Lab, Department of Physics, University of Kashan, Kashan, Iran
E-mail: zhdfr@kashanu.ac.ir

Abstract

An improved mixed order model is presented to describe the thermoluminescence (TL) glow peaks. In this model a fraction of charge carriers, which undergo nonradiative recombination following thermal excitation is taken into account. Therefore, it is expected that the proposed model will produce more realistic kinetic parameters than that of mixed order model. The TL glow curves generated by the proposed model are fitted to the glow curves of general order and mixed order models using a curve fitting program. The results are presented and discussed.

Keywords: Thermoluminescence; improved mixed order model; nonradiative recombination; Kinetics

1. Introduction

The first order kinetics theory of Randall and Wilkins (1945) and second order kinetics of Garlick and Gibson (1948) are the basic phenomenological TL theory. However, there are many experimental glow peaks with shapes that do not correspond to first or second orders of kinetics.

In order to study a general order TL peak whose kinetic order is not necessarily 1 or 2, May and Partridge (1964) presented the general order (GO) of kinetics as follows:

$$I(t) = -\frac{dn}{dt} = \frac{s}{n_o^{b-1}} n^b \exp\left(-\frac{E}{kT}\right) \quad (1)$$

In which $I(\text{cm}^{-3} \text{s}^{-1})$ is the TL intensity, $n(\text{cm}^{-3})$ the concentration of charge carriers in traps, $n_o(\text{cm}^{-3})$ the initial concentration of carriers in traps, $s(\text{s}^{-1})$ the frequency factor, $E(\text{eV})$ the activation energy, $k(\text{eV/K})$ the Boltzman's constant, $T(\text{K})$ the sample temperature and b the order of kinetics which takes values between 1 and 2 and somewhat beyond this range. Despite extensive application of GO model, it cannot be acquired directly by solving the differential equations governing the transport of charge carriers between trapping states, conduction band and recombination centers and the parameter b has no clear physical meaning.

Looking at the practical side, the MO kinetics model is a very interesting one, because it has a clear physical explanation, e.g. all parameters used in the equation are not disputable from the physical point of view. It is more suitable to use this equation for physical analysis of TL process, because the obtained results could be directly connected with real parameters defining the process. The basic equation is more complex than the GO kinetics, but it is simple enough to consider and solve analytically (Chen et al., 1981; Chen and McKeever, 1997).

$$I(t) = -\frac{dn}{dt} = n(n+c)s' \exp\left(-\frac{E}{kT}\right) \quad (2)$$

where $c(\text{cm}^{-3})$ is the concentration of electrons in thermally disconnected deep traps (TDDT) which are stable in the temperature range in which the active traps (AT) are being emptied and $s' = s/(N+c)$. $N(\text{cm}^{-3})$ is the concentration of trapping states. Other parameters are as defined in Eq. (1). By solving Eq. (2), the TL intensity for MO model yields:

$$I(T) = \frac{c^2 s' \alpha \exp\left(-\frac{E}{kT}\right) \exp\left(\frac{cs'}{\beta} \int_{T_0}^T \exp\left(-\frac{E}{kT'}\right) dT'\right)}{\left\{ \exp\left(\frac{cs'}{\beta} \int_{T_0}^T \exp\left(-\frac{E}{kT'}\right) dT'\right) - \alpha \right\}^2} \quad (3)$$

where $\alpha = n_o/(n_o+c)$. It is clear that for $c \gg n$ ($\alpha \approx 0$), Eq. (2) reduces to the first order model and for $c \ll n$ ($\alpha \approx 1$) it approaches to the second order model. Therefore, the MO model includes not only

*Corresponding author

the first and the second order of kinetics, but also intermediate states between the two limiting cases. It is important to note that knowing the value of parameter α of an experimental TL glow peak, leads to the knowledge of the physically meaningful parameter c , while we cannot draw any significant information from the value of b . Yossian and Horowitz (1997) carried out the fitting of glow peak 5 of LiF: Mg, Ti (TLD-100) to MO and GO kinetics expressions of TL. The purpose ostensibly was to explore whether the MO is a better alternative for fitting an experimental TL glow curve than the GO due to the fact that the former has a physical basis, whereas the latter is merely an empirical one. Zahedifar et al. (2007) carried out this study for the TL glow peak 4 of LiF: Mg, Cu, P (GR-200) and came to the conclusion that the MO model takes precedence over the GO model. The advantage of MO model is that it takes into account (via parameter c) the concentration of trapped electrons or holes which do not take part in TL process in the considered temperature range due to their being in deep traps or in low probability recombination centers. However, the other physical reality is that in TL process a fraction of thermally excited electrons to conduction band undergo nonradiative recombination. The aim of this paper is to take into account in TL process the above authenticity and to derive the corresponding TL intensity.

2. Proposed function for the improved mixed order (IMO) model

A generalized scheme which accounts for the multiplicity of trapping states and emission process is shown in Fig. 1.

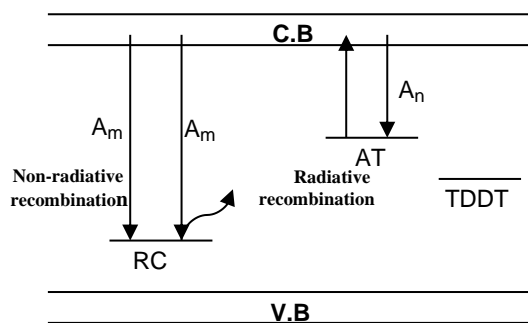


Fig. 1. Level scheme for one trap, one recombination center in presence of thermally disconnected deep trap (TDDT). AT and RC show the active trap and recombination center respectively

At a given temperature, only the traps of one kind are active. All TDDT are assumed to be at one level and all recombination centers (RC) to be of one type. In this model we consider that at time $t=0$, in addition to $n_o(\text{cm}^{-3})$ electrons in AT which finally

recombine with holes in recombination centers and release photons, there are a number of electrons that experience nonradiative recombination and the released energy returns to the lattice vibrations. We show the concentration of these electrons with $u_o(\text{cm}^{-3})$. At a given time t , the above quantities are shown with n and u . Also, $c(\text{cm}^{-3})$ is the concentration of charge carriers in TDDT. Therefore, the rate equations governing the transport of charge carriers during the heating are:

$$-\frac{dm}{dt} = A_m m n c \tag{4}$$

$$-\frac{d(n+u)}{dt} = (n+u) s \exp\left(-\frac{E}{kT}\right) - A_n (N - n - u) n c \tag{5}$$

$$\frac{dn_c}{dt} = \frac{dm}{dt} - \frac{du}{dt} - \frac{dn}{dt} \tag{6}$$

Establishing the so-called quasi equilibrium condition which implies that $|dn_c/dt|$ is negligible compared with $|dn/dt + du/dt|$, results in:

$$\frac{dm}{dt} = \frac{dn}{dt} + \frac{du}{dt} \tag{7}$$

Then:

$$I(t) = -\frac{dn}{dt} \tag{8}$$

We introduce the parameter α_1 as:

$$\alpha_1 = \frac{n_o}{n_o + u_o} \tag{9}$$

It is expected that the ratio u/n in ATs remain unchanged while the sample is being heated, i.e. $u/n = u_o/n_o$. This condition can be expressed as follows:

$$\frac{du}{dt} / \frac{dn}{dt} = \frac{u}{n} \tag{10}$$

Eqs. (9) and (10) immediately yield:

$$\alpha_1 = \frac{n}{n + u} \tag{11}$$

Using Eqs. (10) and (11), Eq. (7) can be written as:

$$\frac{dm}{dt} = \frac{d(n+u)}{dt} = \frac{1}{\alpha_1} \frac{dn}{dt} \tag{12}$$

Combining Eqs. (4), (5) and (12) the expression below yields:

$$-\frac{1}{\alpha_1} \frac{dn}{dt} = (n+u)s \exp\left(-\frac{E}{kT}\right) \times \frac{A_m m}{A_m m + A_n (N - n - u)} \quad (13)$$

Considering $c(\text{cm}^{-3})$ as a constant during the emptying of the ATs, the charge neutrality condition takes the form:

$$m = n + u + c + n_c \quad (14)$$

Neglecting n_c compared with n , u and c results in:

$$m = n + u + c \quad (15)$$

In order to obtain an analytical solution for the differential equations describing the proposed IMO, it is assumed that $A_m = A_n$. This assumption has also been considered to obtain the TL intensity of the original mixed order model of Chen et al. (1981). Changing the variable from t to $T = T_o + \beta t$ where β (Ks^{-1}) is the heating rate, t (s) is the time and T_o (K) the initial temperature of the sample and substituting m from Eq. (15) in Eq. (13), we have:

$$-\beta \frac{dn}{dT} = \frac{1}{\alpha_1} n(n + \alpha_1 c) s' \exp\left(-\frac{E}{kT}\right) \quad (16)$$

where $s' = s / (N + c)$ and $N(\text{cm}^{-3})$ is the concentration of active electron traps. Solving the differential equation (16) for obtaining n as a function of T results in:

$$n = \frac{\frac{\alpha_1 \alpha_2 c}{\alpha_1 + \alpha_2 - \alpha_1 \alpha_2}}{\exp\left(\frac{cs'}{\beta} \int_{T_o}^T \exp\left(-\frac{E}{kT'}\right) dT'\right) - \frac{\alpha_2}{\alpha_1 + \alpha_2 - \alpha_1 \alpha_2}} \quad (17)$$

where $\alpha_2 = n_o / (n_o + c)$ is familiar from the MO model. Inserting n from Eq. (17) in Eq. (8) and changing the variable from t to $T = T_o + \beta t$, the TL intensity for the IMO model takes the following form:

$$I(T) = \frac{c^2 s' \alpha_1 \alpha_2}{\alpha_1 + \alpha_2 - \alpha_1 \alpha_2} \times \exp\left(-\frac{E}{kT}\right) \exp\left(\frac{cs'}{\beta} \int_{T_o}^T \exp\left(-\frac{E}{kT'}\right) dT'\right) \times \left\{ \exp\left(\frac{cs'}{\beta} \int_{T_o}^T \exp\left(-\frac{E}{kT'}\right) dT'\right) - \frac{\alpha_2}{\alpha_1 + \alpha_2 - \alpha_1 \alpha_2} \right\}^{-2} \quad (18)$$

Using the approximation below (Kitis et al., 1998):

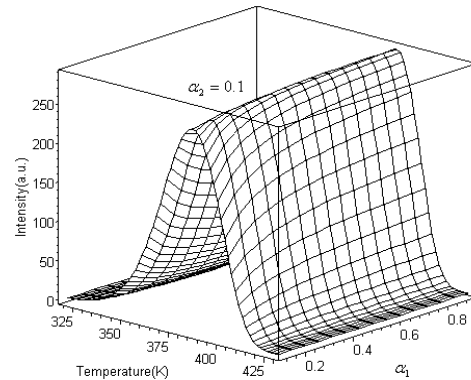
$$\int_{T_o}^T \exp\left(-\frac{E}{kT'}\right) dT' = \frac{kT^2}{E} \exp\left(-\frac{E}{kT}\right) \left(1 - \frac{2kT}{E}\right) \quad (19)$$

The analytical equation for this model is obtained as:

$$I(T) = \frac{c^2 s' \alpha_1 \alpha_2}{\alpha_1 + \alpha_2 - \alpha_1 \alpha_2} \exp\left(-\frac{E}{kT}\right) \times \exp\left(\frac{cs' kT^2}{\beta E} \exp\left(-\frac{E}{kT}\right) \left(1 - \frac{2kT}{E}\right)\right) \times \left\{ \exp\left(\frac{cs' kT^2}{\beta E} \exp\left(-\frac{E}{kT}\right) \left(1 - \frac{2kT}{E}\right)\right) - \frac{\alpha_2}{\alpha_1 + \alpha_2 - \alpha_1 \alpha_2} \right\}^{-2} \quad (20)$$

3. Results and comparisons

It is a simple task to show that in the case of $u_o = 0$ which corresponds to $\alpha_1 = 1$, the proposed model reduces to the usual mixed order model (Eq. 3). Also in the other limiting case of $\alpha_1 \approx 0$ (equivalent to $n_o = 0$) which means that all the trapped charge carriers undergo nonradiative recombination, the TL intensity approaches zero as is expected. Fig. 2 (a, b, c) shows the synthetic glow curves generated using IMO model for different values of α_1 and α_2 parameters.



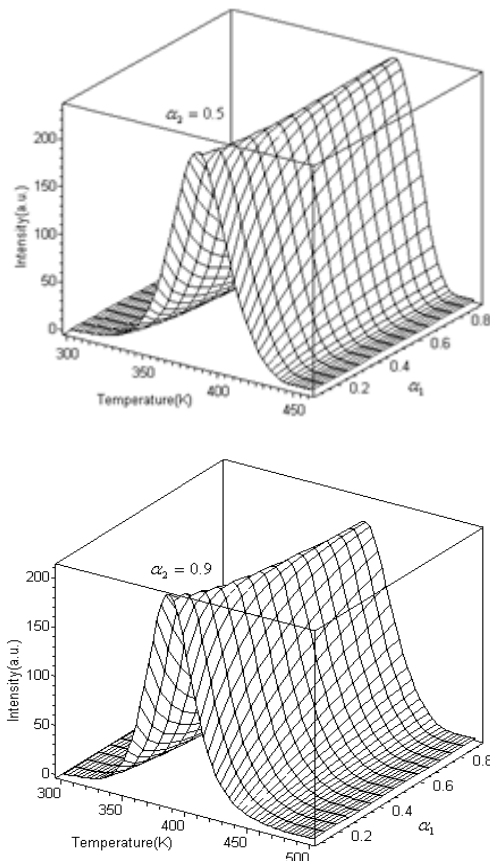


Fig. 2(a, b, c) Three-dimensional plots of IMO glow peaks for (a) $\alpha_1=0.1$, (b) $\alpha_1=0.5$ and (c) $\alpha_1=0.9$ and using Eq. 20

These figures have been generated using constant values of $N=1e13 \text{ (cm}^{-3}\text{)}$, $n_o = 1e12 \text{ (cm}^{-3}\text{)}$, $s=1e12 \text{ (s}^{-1}\text{)}$, $E=1 \text{ (eV)}$ and $\beta=1 \text{ (Ks}^{-1}\text{)}$. The glow peaks produced by the proposed model were compared to those of MO (Eq. 3) and GO (Eq. 1) models by fitting the GO and MO glow peaks to the synthetic glow peaks generated by IMO model. Table 1 shows 36 pairs of the parameters α_1 and α_2 used to create the glow peaks of IMO expression (Eq. 20). In each 6 consecutive lines, the parameter α_1 remains fixed, while the parameter α_2 varies between 0 and 1, so a broad range of the pairs α_1 and α_2 are taken into consideration. Tables 2, 3 show the results of fitting the MO and GO models (Eqs. 3, 1) to the synthetic IMO glow peaks of Table 1.

A computer program developed in our laboratory using Levenberg-Marquart algorithm based on non-linear least square method was employed to fit the TL glow curves of GO and MO model to the synthetic glow curves produced by IMO model (Eq. 20). For testing the goodness of fit, the figure of merit (FOM) was used:

$$FOM(\%) = \sum_{j_f}^{j_l} \frac{100|y_i - y(x_i)|}{A} \tag{21}$$

Table 1. 36 pairs of the parameters α_1 and α_2 used to generate the glow peaks of IMO expression (Eq.20). In each 6 consecutive lines, the parameter α_1 remains fixed, while the parameter α_2 varies between 0 and 1. Other parameters are $n_o=1e12 \text{ (cm}^{-3}\text{)}$, $N=1e13 \text{ (cm}^{-3}\text{)}$ (for line numbers 1 to 6, $N=1e14 \text{ (cm}^{-3}\text{)}$), $s=1e12 \text{ (s}^{-1}\text{)}$, $E=1 \text{ (eV)}$, $\beta=1 \text{ (K/s)}$

L.N.	Parameters		L.N.	Parameters	
	α_1	α_2		α_1	α_2
1	0.01	0.01	19	0.60	0.01
2	0.01	0.20	20	0.60	0.20
3	0.01	0.40	21	0.60	0.40
4	0.01	0.60	22	0.60	0.60
5	0.01	0.80	23	0.60	0.80
6	0.01	0.99	24	0.60	0.99
7	0.20	0.01	25	0.80	0.01
8	0.20	0.20	26	0.80	0.20
9	0.20	0.40	27	0.80	0.40
10	0.20	0.60	28	0.80	0.60
11	0.20	0.80	29	0.80	0.80
12	0.20	0.99	30	1.00	0.99
13	0.40	0.01	31	1.00	0.01
14	0.40	0.20	32	1.00	0.20
15	0.40	0.40	33	1.00	0.40
16	0.40	0.60	34	1.00	0.60
17	0.40	0.80	35	1.00	0.80
18	0.40	0.99	36	1.00	0.99

In which j_f and j_l are the numbers of the first and last temperature interval ΔT used for curve fitting, y_i is the intensity in the i th interval obtained from IMO model and $y(x_i)$ the intensity produced by MO and GO models, and A the total area of fitted glow peak between j_f and j_l . The lower FOM value corresponds to a better fit (Balian and Eddy, 1977). As is apparent in Table 2, only for line numbers (L.Ns) 31-36, where α_1 takes the maximum value of 1, MO model entirely coincides to generated IMO glow peaks.

Table 2. Fitted parameters of MO model (Eq. 3) to the synthetic IMO glow peaks of Table 1. Except the parameters α_1 and α_2 which differ in each line of Table 1, other input parameters used to generate the TL glow peaks of IMO model are $n_o=1e12$ (cm^{-3}), $N=1e13$ (cm^{-3}) (for line numbers 1 to 6, $N=1e14$ (cm^{-3})), $s=1e12$ (s^{-1}), $E=1$ (eV), $\beta=1$ (K/s)

L.N.	Fitted parameters in MO					
	α	$N(cm^{-3})$	$n_o(cm^{-3})$	$s(s^{-1})$	$E(eV)$	$FOM(\%)$
1	0.01	1.00×10^{14}	1.00×10^{12}	1.50×10^{10}	0.85	4.70
2	0.20	1.00×10^{14}	1.00×10^{12}	1.61×10^{09}	0.70	15.8
3	0.40	1.00×10^{14}	1.00×10^{12}	1.24×10^{10}	0.75	15.3
4	0.60	1.00×10^{14}	1.00×10^{12}	1.33×10^{11}	0.81	13.1
5	0.80	1.00×10^{14}	1.00×10^{12}	2.57×10^{12}	0.89	9.04
6	0.99	1.00×10^{14}	1.00×10^{12}	8.60×10^{13}	0.99	0.66
7	0.01	1.00×10^{13}	1.00×10^{12}	7.45×10^{11}	0.99	0.25
8	0.20	1.00×10^{13}	1.00×10^{12}	3.60×10^{10}	0.88	4.15
9	0.40	1.00×10^{13}	1.00×10^{12}	1.94×10^{10}	0.84	6.73
10	0.60	1.00×10^{13}	1.00×10^{12}	4.05×10^{10}	0.86	7.69
11	0.80	1.00×10^{13}	1.00×10^{12}	2.68×10^{11}	0.91	6.37
12	0.99	1.00×10^{13}	1.00×10^{12}	4.42×10^{12}	1.00	0.61
13	0.01	1.00×10^{13}	1.00×10^{12}	8.94×10^{11}	1.00	0.09
14	0.20	1.00×10^{13}	1.00×10^{12}	1.93×10^{11}	0.94	1.81
15	0.40	1.00×10^{13}	1.00×10^{12}	9.72×10^{10}	0.91	3.39
16	0.60	1.00×10^{13}	1.00×10^{12}	1.10×10^{11}	0.91	4.43
17	0.80	1.00×10^{13}	1.00×10^{12}	3.10×10^{11}	0.94	4.18
18	0.99	1.00×10^{13}	1.00×10^{12}	2.28×10^{12}	1.00	0.46
19	0.01	1.00×10^{13}	1.00×10^{12}	9.51×10^{11}	1.00	0.04
20	0.20	1.00×10^{13}	1.00×10^{12}	4.40×10^{11}	0.97	0.85
21	0.40	1.00×10^{13}	1.00×10^{12}	2.79×10^{11}	0.95	1.70
22	0.60	1.00×10^{13}	1.00×10^{12}	2.66×10^{11}	0.95	2.40
23	0.80	1.00×10^{13}	1.00×10^{12}	4.47×10^{11}	0.96	2.47
24	0.99	1.00×10^{13}	1.00×10^{12}	1.57×10^{12}	1.00	0.30
25	0.01	1.00×10^{13}	1.00×10^{12}	9.81×10^{11}	1.00	0.02
26	0.20	1.00×10^{13}	1.00×10^{12}	7.21×10^{11}	0.99	0.33
27	0.40	1.00×10^{13}	1.00×10^{12}	5.83×10^{11}	0.98	0.68
28	0.60	1.00×10^{13}	1.00×10^{12}	5.50×10^{11}	0.98	1.01
29	0.80	1.00×10^{13}	1.00×10^{12}	6.71×10^{11}	0.98	1.11
30	0.99	1.00×10^{13}	1.00×10^{12}	1.21×10^{12}	1.00	1.14
31	0.01	1.00×10^{13}	1.00×10^{12}	1.00×10^{12}	1.00	0.00
32	0.20	1.00×10^{13}	1.00×10^{12}	1.00×10^{12}	1.00	0.00
33	0.40	1.00×10^{13}	1.00×10^{12}	1.00×10^{12}	1.00	0.00
34	0.60	1.00×10^{13}	1.00×10^{12}	1.00×10^{12}	1.00	0.00
35	0.80	1.00×10^{13}	1.00×10^{12}	1.00×10^{12}	1.00	0.00
36	0.99	1.00×10^{13}	1.00×10^{12}	1.00×10^{12}	1.00	0.00

Table 3. Fitted parameters of GO model (Eq. 1) to the synthetic IMO glow peaks of Table 1. Except the parameters α_1 and α_2 which differ in each line of Table 1, other input parameters used to generate the TL glow peaks of IMO model are $n_o=1e12 (cm^{-3})$, $N=1e13 (cm^{-3})$ (for line numbers 1 to 6, $N=1e14 (cm^{-3})$), $s=1e12(s^{-1})$, $E=1(eV)$, $\beta=1 (K/s)$

L.N.	Fitted parameters in GO				
	b	$n_o(cm^{-3})$	$s(s^{-1})$	$E(eV)$	$FOM(\%)$
1	1.16	1.01×10^{12}	6.57×10^{10}	0.92	2.54
2	1.90	1.01×10^{12}	4.97×10^{11}	0.98	1.74
3	1.97	1.00×10^{12}	8.12×10^{11}	0.99	0.77
4	1.99	1.00×10^{12}	9.36×10^{11}	1.00	0.35
5	2.00	1.00×10^{12}	9.85×10^{11}	1.00	0.13
6	2.00	1.00×10^{12}	1.00×10^{12}	1.00	0.00
7	1.01	1.00×10^{12}	7.10×10^{11}	0.99	0.21
8	1.20	1.01×10^{12}	3.68×10^{10}	0.91	2.82
9	1.43	1.01×10^{12}	3.30×10^{10}	0.91	3.50
10	1.66	1.01×10^{12}	7.28×10^{10}	0.94	3.27
11	1.87	1.01×10^{12}	2.16×10^{11}	0.97	1.96
12	2.00	1.00×10^{12}	4.97×10^{11}	1.00	0.03
13	1.00	1.00×10^{12}	8.00×10^{11}	0.99	0.11
14	1.10	1.01×10^{12}	5.36×10^{10}	0.93	1.88
15	1.25	1.01×10^{12}	1.81×10^{10}	0.91	3.17
16	1.46	1.01×10^{12}	1.96×10^{10}	0.91	3.66
17	1.73	1.01×10^{12}	5.51×10^{10}	0.95	2.89
18	2.00	1.00×10^{12}	2.45×10^{11}	1.00	0.09
19	1.00	1.00×10^{12}	2.45×10^{11}	1.00	0.08
20	1.07	1.01×10^{12}	7.45×10^{10}	0.95	1.40
21	1.18	1.01×10^{12}	1.85×10^{10}	0.91	2.65
22	1.35	1.01×10^{12}	1.18×10^{10}	0.91	3.53
23	1.63	1.01×10^{12}	2.37×10^{10}	0.93	3.37
24	1.99	1.00×10^{12}	1.60×10^{11}	1.00	0.19
25	1.00	1.00×10^{12}	8.52×10^{11}	1.00	0.05
26	1.05	1.00×10^{12}	9.39×10^{10}	0.96	1.11
27	1.13	1.01×10^{12}	2.12×10^{10}	0.92	2.26
28	1.28	1.01×10^{12}	9.67×10^9	0.91	3.29
29	1.54	1.01×10^{12}	1.35×10^{10}	0.92	3.57
30	1.99	1.00×10^{12}	1.18×10^{11}	1.00	0.25
31	1.00	1.00×10^{12}	8.63×10^{11}	1.00	0.04
32	1.04	1.00×10^{12}	1.11×10^{11}	0.96	0.92
33	1.11	1.01×10^{12}	2.45×10^{10}	0.93	1.96
34	1.23	1.01×10^{12}	9.11×10^9	0.91	3.04
35	1.48	1.01×10^{12}	9.18×10^9	0.92	3.64
36	1.99	1.00×10^{12}	9.19×10^{10}	1.00	0.31

The obtained value of zero for FOM shows such a correspondence, while for the least value of 0.01 assumed for α_1 , (L.N.1-6) which corresponds to the

maximum rate of nonradiative transitions, the mismatch between MO and IMO models is significant and the FOM takes its largest values. In other L. Ns., MO model does not coincide to

generated IMO glow peaks and this mismatch is larger for lower values of α_1 . As is apparent in Table 1, six values for α_1 have been assumed between 0.01-1 and for each α_1 , the parameter α_2 takes the values of 0.01, 0.2, 0.4, 0.6, 0.8 and 0.99, forming totally six groups. In each groups, the FOM obtained in fitting the MO glow peaks to the generated IMO glow peaks has lower values for low and high values of α_2 , and takes the maximum value in the middle of each group. The values for α , N and n_o were assumed the same for IMO and MO glow peaks. The fitted values of s and E for small values of the parameter α_1 differ from those of IMO model; however, with the parameter α_1 approaching to 1, the s and E values of two models come close to each other. This is expectable because with closing the parameter α_1 to its upper value of 1, the concentration of charge carriers u_o goes to zero, thus the proposed IMO model reduces to the MO model.

Shown in Table 3 are the fitted values of GO model to the 36 generated IMO glow peaks of Table 1. FOM values demonstrate that the glow peaks of GO model do not fairly match those of the IMO model. The fitted values of E and s are also different from the analogous parameters of IMO model, while the n_o values of two models remain close to each other. It is seen however that FOM values take the smallest amounts when the order of kinetics b is equal to its limiting values of 1 and 2. The reason is that the parameters α_1 and α_2 are taken to be constant in the temperature interval of the glow peak whereas b (despite the fact that it is assumed constant in the GO model) changes with raising the temperature in the region that the glow peak appears, except for limiting values of $b=1, 2$ (Yossian and Horowitz, 1997; Sunta, 2002). Fig.3 (a, b) are obtained for L.N.5 and L.N.10 where the GO model (Eq. 1) and MO model (Eq. 3) are fitted to the IMO model. Fig. 4 shows the variation of the symmetry factor (defined as $\mu_g = (T_2 - T_m)/(T_2 - T_1)$ in which T_2 and T_1 are higher and lower half-maximum intensity temperatures and T_m is the maximum temperature) with parameter α_2 for different values of $\alpha_1=0.1, 0.3, 0.5, 0.7, 1$. Peak parameters used to produce the glow peaks are $n_o = 1 \times 10^{10} (cm^{-3})$, $N = 1 \times 10^{15} (cm^{-3})$, $s = 1 \times 10^{10} (s^{-1})$, $\beta = 5 (K/s)$ and $E = 1 (eV)$. The curve corresponding to $\alpha_1=1$ ($u_o = 0$) is familiar to the mixed order model (Kitis, 2000). (a)

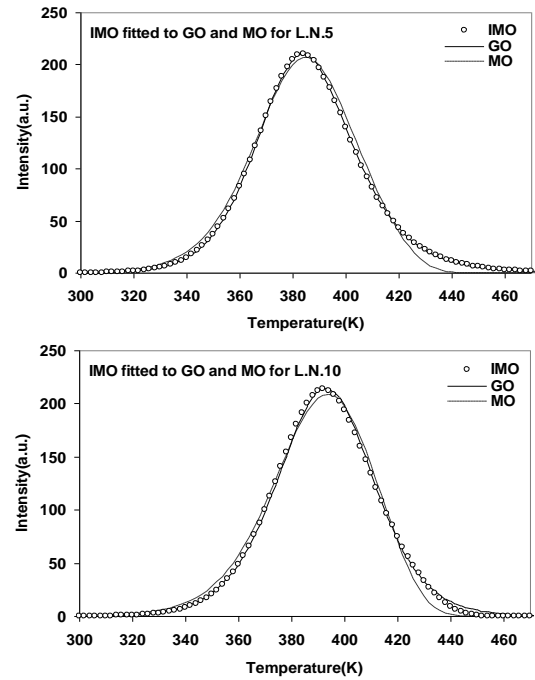


Fig. 3(a, b) GO glow peaks (solid curves) and MO glow peaks (dashed curves) fitted to the simulated IMO glow peaks (open circles) for (a) L.N.5 and (b) L.N.10 of Table 1

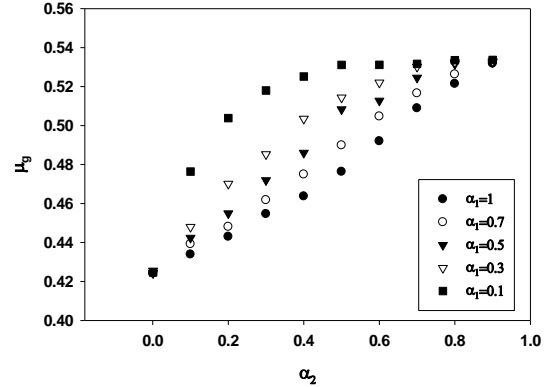


Fig. 4. Variation of the symmetry factor, $\mu_g = (T_2 - T_m)/(T_2 - T_1)$ with parameter α_2 for different values of $\alpha_1=0.1, 0.3, 0.5, 0.7, 1$. Peak parameters used to produce the glow peaks are $n_o = 1 \times 10^{10} (cm^{-3})$, $N = 1 \times 10^{15} (cm^{-3})$, $s = 1 \times 10^{10} (s^{-1})$, $\beta = 5 (K/s)$ and $E = 1 (eV)$

As shown, in the two limiting cases of $\alpha_2 = 0$ and $\alpha_2 = 1$, the variation of α_1 does not affect the symmetry factor, but in the intermediate values of α_2 the symmetry factor is a sensitive function of α_1 . It is notable that for a given value of the parameter α_2 , an increase in u_o (decrease in α_1) reduces the rate of radiative recombination and causes the rate

of retrapping to overcome the recombination rate. At the limiting values of $\alpha_2 = 0$ and $\alpha_2 = 1$ as is apparent from Eq. (18), the TL intensity is independent of the parameter α_1 , but between the two limiting values, a decrease in the parameter α_1 causes the retrapping to prevail over recombination and consequently the symmetry factor to approach to the higher values. Table 3 in which the GO glow peaks are fitted to the IMO glow peaks can also be employed for more clarification. It is seen in this table that for a fixed value of α_2 (e.g. $\alpha_2 = 0.4$) and different values of $\alpha_1 = 1, 0.8, 0.6, 0.4, 0.2, 0.01$ which correspond to the line numbers of 33, 27, 21, 15, 9, 3 respectively, with decreasing the parameter α_1 , the fitted GO glow peaks go towards the second order glow peaks and the fitted values of the kinetic order b shift towards upper limiting value of 2.

4. Conclusion

One advantage of the MO model (Eq. 3) compared to the general order model (Eq. 1) is that it is more physical and the parameter α in Eq. 3 informs us of the meaningful parameter c , while the basis of the parameter b in general order model is empirical. The presented model is more physical, i.e. the fraction of charge carriers which do not take part in TL and undergo nonradiative recombination are taken into consideration via the parameter α_1 . By solving the differential equations describing the phenomenon, an analytical expression was derived for the TL intensity and the behavior of presented model was checked in limiting cases of $\alpha_1 = 0$ and $\alpha_1 = 1$. Taking into consideration that the proposed model reduces to the usual mixed order model in the limiting case of $\alpha_1 \approx 1$ ($u_0 \approx 0$), it results in the present model with an additional adjustable parameter α_1 being more compatible with the experimental glow peaks than the MO model.

References

- Balian, H. G., & Eddy, N. W. (1977). Figure-of-merit (FOM), an improved criterion over the normalized chi-squared test for assessing goodness-of-fit of gamma-ray spectral peaks. *Nuclear Instruments and Methods*, 145(2), 389–395.
- Chen, R., Kristianpoller, N., Davidson, Z., & Visocekas, R. (1981). Mixed first and second order kinetics in thermally stimulated processes. *Journal of Luminescence*, 23(3-4), 293–303.
- Chen, R., & McKeever, S. W. S. (1997). *Theory of thermoluminescence and related phenomena*. World Scientific, Singapore.
- Garlick, G. F. J., & Gibson, A. F. (1948). The electron trap mechanism of luminescence in sulphide and silicate phosphors. *Proceedings of the Physical Society*, 60(6), 574–589.
- Kitis, G., & Gomez-Ros, J. M. (2000). Thermoluminescence glow-curve deconvolution function for mixed order of kinetics and continuous trap distribution. *Nuclear Instruments and Methods in Physics Research Section A*, 440(1), 224–231.
- Kitis, G., Gomez-Ros, J. M., & Tuyn, J. W. N. (1998). Thermoluminescence glow-curve deconvolution function for first, second and general order of kinetics. *Journal of Physics D: Applied Physics*, 31(19), 2636–2641.
- May, C. E., & Partridge, J. A. (1964). Thermoluminescence kinetics of alpha irradiated alkali halides. *The Journal of Chemical Physics*, 40, 1401–1415.
- Randall, J. T., & Wilkins, M. H. F. (1945a). Phosphorescence and electron traps: I. The study of trap distribution. *Proceedings of the Royal Society (London) A*, 184, 366–389.
- Sunta, C. M., Ayta, W. E. F., Chubaci, J. F. D., & Watanabe, S. (2002). General order and mixed order fits of thermoluminescence glow curves—a comparison. *Radiation Measurements*, 35(1), 47–57.
- Yossian, D., & Horowitz, Y. S. (1997). Mixed-order and general-order kinetics applied to synthetic glow peaks and to peak 5 in LiF:Mg,Ti (TLD-100). *Radiation Measurements*, 27(3), 465–471.
- Zahedifar, M., Kavianinia, M. J., & Ahmadi, M. (2007). Effect of population of trapping states on kinetic parameters of LiF: Mg, Cu, P(GR-200) using mixed and general order of kinetics. *Radiation Measurements*, 42(4–5), 815–818.